Comp. & Maths. with Appls. Vol. 6, pp. 213–233
Pergamon Press Ltd., 1980. Printed in Great Britain

STAGNATION FLOWS OF MICROPOLAR FLUIDS WITH STRONG AND WEAK INTERACTIONS

G. S. GURAM† and A. C. SMITH
Department of Mathematics, University of Windsor, Ontario, Canada N9B 3P4

Communicated by I. N. Sneddon

(*Received March* 1979)

Abstract—Plane and axially symmetric flows of a micropolar fluid, in contact with an infinite plate, and tending to potential flow at infinity, with a stagnation point on the plate, are considered. Two different boundary conditions for the spin are considered: (a), vanishing spin; and (b), vanishing surface moment. The equations of motion are reduced to dimensionless forms which include three dimensionless parameters, and integrated numerically by a Runge–Kutta method. Results are presented both in tabular and graphical form, and the effects of the values of the parameters on the flow are discussed.

1. INTRODUCTION AND SUMMARY

Stagnation flow of a micropolar fluid has been treated by Peddieson and McNitt[1], who considered both plane and axisymmetric flows, using boundary layer theory, with the condition that the spin should vanish on the solid boundary. Peddieson[2] later applied the micropolar model to turbulent shear flow, and used a boundary condition analogous to the vanishing of the eddy viscosity, namely, that the spin should be equal to the velocity gradient.

Recently Ahmadi[3] obtained self-similar solutions of the boundary layer equations for micropolar flow, imposing the restriction that $(\mu + (1/2)\kappa)j = \gamma$ and requiring that $2\phi + u_y = 0$ on the solid boundary (see Section 2 for notation), while allowing the material coefficients γ and j to vary. The equations obtained contain two parameters, $K = \kappa/\mu$, and I, taken equal to unity.

Ebert[4] considered boundary layer flow with the condition that the spin should vanish on the boundary.

The correct boundary condition to be applied to the spin is still an open question. Several have been proposed in literature (see[5–7]), the most common of which is the vanishing of the spin on the boundary; the so-called "strong" interaction. The opposite extreme, the "weak" interaction, is the vanishing of the moment stress on the boundary. A third, or "compromise" is the vanishing of a linear combination of spin, shearing stress and couple stress, involving some friction co-efficients, a particular case of which was the condition used by Peddieson[2].

It should be noted that the condition $g'(0) = 0$ used in Section 3 has implications different from the same condition formally used by Ahmadi. The latter is a consequence of the boundary layer equations and initial values ([3], 3.10–13). The former derives from the vanishing of the moment stress on the boundary, and indeed, the condition $m_{23} = 0$ on $y = 0$ does not imply $2\phi + u_y = 0$ on $y = 0$ (see Section 6).

In this paper we follow the classical treatment of stagnation flow ([8], p. 87), assuming potential flow with complex potential $w = (1/2)az^2$ far from the boundary. The two extreme boundary conditions will be considered: (a) the vanishing of the spin, and (b) the vanishing of the spin gradient, in the case of steady plane and axisymmetric flows with a stagnation point. In Section 2, the basic equations are given. In Section 3, we reduce the equations of motion to two nonlinear ordinary differential equations, in dimensionless form, involving three parameters. These equations are then integrated numerically, using a fourth-order Runge–Kutta method (Section 4). The axially symmetric case is likewise considered (Section 5). Results are presented in tabular and graphical form, and discussed in Section 6.

2. EQUATIONS OF MOTION

The equations of motion of a micropolar fluid, with isotropic microstructure, are[7]

†Present address: Department of Applied Mathematics, University of Western Ontario, London, Ontario, Canada.

$$
\begin{aligned}
&(\lambda + 2\mu + \kappa)\nabla(\nabla \cdot \mathbf{v}) - (\mu + \kappa)\nabla \times \nabla \times \mathbf{v} \\
&\quad + \kappa \nabla \times \boldsymbol{\nu} - \nabla p + \rho \mathbf{f} = \rho \dot{\mathbf{v}}, \\
&(\alpha + \beta + \gamma)\nabla(\nabla \cdot \boldsymbol{\nu}) - \gamma(\nabla \times \nabla \times \boldsymbol{\nu}) + \kappa \nabla \times \mathbf{v} \\
&\quad - 2\kappa \boldsymbol{\nu} + \rho \mathbf{l} = \rho j \dot{\boldsymbol{\nu}} \\
&\qquad \dot{\rho} + \rho(\nabla \cdot \mathbf{v}) = 0,
\end{aligned}
\tag{2.1}
$$

where $\mathbf{v}$ is the velocity, $\boldsymbol{\nu}$ the micro-rotation, or spin, p the thermodynamic pressure, $\mathbf{f}$ and $\mathbf{l}$ the body-force and -couple per unit mass, ρ the density and j the micro-inertia; λ, μ, κ, α, β and γ are material constants, or viscosity coefficients; and the dot signifies material differentiation.

The constitutive equations giving t_{kl}, the stress tensor, and m_{kl}, the couple stress tensor are, in cartesian co-ordinates,

$$
\begin{aligned}
t_{kl} &= (-p + \lambda v_{r,r})\delta_{kl} + \mu(v_{k,l} + v_{l,k}) + \kappa(v_{l,k} - e_{klr}\nu_r), \\
m_{kl} &= \alpha \nu_{r,r}\delta_{kl} + \beta \nu_{k,l} + \gamma \nu_{l,k},
\end{aligned}
\tag{2.2}
$$

where δ_{kl} and e_{klm} are the Kronecker delta and the alternating symbol respectively; the summation convention has been used; and the comma denotes partial differentiation with respect to a space co-ordinate.

The stress vector, $\mathbf{T}$, and moment stress vector $\mathbf{M}$, across a surface element with unit normal $\mathbf{n}$ are given by

$$
T_k = t_{lk} n_l, \qquad M_k = m_{lk} n_l. \tag{2.3}
$$

The material constants must satisfy the inequalities

$$
\begin{aligned}
&3\lambda + 2\mu + \kappa \geq 0, \qquad 2\mu + \kappa \geq 0, \qquad \kappa \geq 0, \\
&3\alpha + \beta + \gamma \geq 0, \qquad \gamma \geq |\beta|;
\end{aligned}
\tag{2.4}
$$

conditions which are necessary and sufficient to ensure that the rate of dissipation of energy should be non-negative.

3. TWO-DIMENSIONAL STAGNATION FLOW

Consider two-dimensional steady flow in the upper half-plane $y > 0$. *Ideal* fluid flow, with a stagnation point at the origin is given by the complex potential $w = (1/2)az^2$, the speed being $q = a(x^2 + y^2)^{1/2}$ and the pressure $p = p_0 - (1/2)\rho a^2(x^2 + y^2)$. When the fluid is *viscous*, bounded below by the infinite plate $y = 0$, and when the flow tends to the potential flow just mentioned as $y \to \infty$, we write (see [8], pp. 88–89)

$$
u = xf'(y), \qquad v = -f(y) \tag{3.1}
$$

satisfying the condition of incompressibility. Then it is found that

$$
u = axh'(\eta), \qquad v = -(a\nu)^{1/2} h(\eta) \tag{3.2}
$$

where $\eta = (a/\nu)^{1/2} y$, $\nu = (\mu/\rho)$, $f(y) = \sqrt{(a\nu)}\, h(\eta)$, and $h(\eta)$ satisfies Hiemenz' equation

$$
h'''(\eta) + h(\eta)h''(\eta) - h'^2(\eta) + 1 = 0 \tag{3.3}
$$

where the prime denotes differentiation with respect to η, with boundary conditions

$$
h(0) = h'(0) = 0, \qquad h'(\infty) = 1. \tag{3.4}
$$

It has been found that the solution is such that $h''(0) = 1.2326$.

Consider now the steady incompressible flow of a *micropolar* fluid in the upper half plane, bounded by the plate $y = 0$, which tends to the flow with potential $w = (1/2)az^2$ as $y \to \infty$.

Let

$$\mathbf{v} = (u(x, y), v(x, y), 0),$$
$$\boldsymbol{\nu} = (0, 0, \phi(x, y)), \tag{3.5}$$

then (2.1) reduce to

$$\begin{aligned}(\mu + \kappa)\nabla^2 u + \kappa\phi_y - p_x &= \rho(uu_x + vu_y)\\ (\mu + \kappa)\nabla^2 v - \kappa\phi_x - p_y &= \rho(uv_x + vv_y)\\ \gamma\nabla^2\phi + \kappa(v_x - u_y) - 2\kappa\phi &= \rho j(u\phi_x + v\phi_y)\\ u_x + v_y &= 0.\end{aligned} \tag{3.6}$$

The subscripts x and y signify partial derivatives and $\nabla^2 \equiv (\partial/\partial x)^2 + (\partial/\partial y)^2$.

Let

$$u = AxF'(y), \qquad v = -AF(y), \qquad \phi = BxG(y), \tag{3.7}$$

then it is found from (3.6) that p_x/x and p_y are functions of y only, and that

$$\frac{\mu + \kappa}{\rho} AF''' + A^2(FF'' - F'^2) + \frac{\kappa}{\rho} BG' = c \tag{3.8}$$

$$\frac{p - p_0}{\rho} = \frac{1}{2}[cx^2 - A^2F^2] - \frac{\mu + \kappa}{\rho} AF' - \frac{\kappa B}{\rho}\int_0^y G(s)\,ds \tag{3.9}$$

$$\gamma BG'' - \kappa AF'' - 2\kappa BG = \rho jAB[F'G - FG'] \tag{3.10}$$

where the prime denotes differentiation with respect to y, p_0 is the stagnation pressure, and c is a constant.

The condition $u = v = 0$ on $y = 0$ requires that

$$F(0) = F'(0) = 0. \tag{3.11}$$

The right hand side of (3.9) tends to the potential flow value $-(1/2)a^2(x^2 + y^2)$ as $y \to \infty$ provided that

$$c = -a^2 \qquad \text{and} \qquad F'(\infty) = a. \tag{3.12}$$

Equations (3.8) and (3.10) can be expressed in terms of dimensionless parameters and variable as follows.

Let

$$u = axf'(\eta), \qquad v = -\lambda af(\eta), \qquad \phi = \frac{\rho a^2\lambda}{\kappa} xg(\eta), \tag{3.13}$$

where

$$\eta = \frac{y}{\lambda} \qquad \text{and} \qquad \lambda^2 = \frac{\mu + \kappa}{\rho a}. \tag{3.14}$$

Equations (3.8) and (3.10) reduce to the forms:

$$\begin{aligned}f'''(\eta) + f(\eta)f''(\eta) - f'^2(\eta) + g'(\eta) + 1 &= 0\\ g''(\eta) - c_1 f''(\eta) - 2c_2 g(\eta) &= c_3(f'(\eta)g(\eta) - f(\eta)g'(\eta))\end{aligned} \tag{3.15}$$

where the prime denotes differentiation with respect to η, and

$$c_1 = \frac{\kappa^2}{\gamma\rho a}, \qquad c_2 = \frac{(\mu+\kappa)\kappa}{\gamma\rho a}, \qquad c_3 = \frac{(\mu+\kappa)j}{\gamma}. \tag{3.16}$$

The constants c_1, c_2, c_3 and the variables η, $f(\eta)$, $f'(\eta)$ and $g(\eta)$ are dimensionless.† The boundary conditions, assuming that $u = v = 0$ on $y = 0$, and potential flow as $y \to \infty$, are

$$f(0) = f'(0) = 0, \qquad f'(\infty) = 1, \qquad g(\infty) = 0. \tag{3.17}$$

An additional condition is required. That most commonly adopted has been the vanishing of the spin on a solid boundary (see [7]), namely

$$g(0) = 0. \tag{3.18}$$

Others which have been proposed (see [5, 6]) are (a) the vanishing of the spin gradient, and hence the tangential component of the moment stress on the boundary; in this case $g'(0) = 0$, and (b) a compromise condition of the form

$$g(0) + pg'(0) + qf''(0) = 0$$

where p and q are friction coefficients, a particular case of which has been considered by Peddieson[2] by setting $\phi = u_y$ on $y = 0$, deduced from an analogy with the vanishing of eddy viscosity on the boundary in turbulent shear flow. We consider here the cases $g(0) = 0$ and $g'(0) = 0$.

4. NUMERICAL INTEGRATION OF EQUATIONS

Equations (3.15), generalisations of Hiemenz' equation, being nonlinear, do not lend themselves readily to analytical solution. A fourth-order Runge–Kutta method was used (see [9], pp. 87–88), writing the equations as a system of five first-order equations. The boundary conditions, being divided between 0 and ∞, necessitated the use of a "shooting" method. Three pairs of values of $f''(0)$ and $g'(0)$ (or $g(0)$) were assumed in addition to the known values $f(0) = f'(0) = 0$, and $g(0) = 0$ (or $g'(0) = 0$), and values of $f'(\infty)$ and $g(\infty)$ obtained. It was found that $\eta = \infty \doteqdot 4$). It was then assumed that $f'(\infty)$ and $g(\infty)$ were linearly dependent on the initial values, and inverse interpolation used to find values of $f''(0)$ and $g'(0)$ (or $g(0)$) which would make $f'(\infty) = 1$ and $g(\infty) = 0$. The method was then repeated until a preassigned accuracy was attained.

5. AXIALLY SYMMETRIC FLOW

Using cylindrical polar co-ordinates, and assuming flow symmetric about the z-axis, with

$$v_r = u(r, z), \qquad v_z = w(r, z), \qquad v_\theta = \phi(r, z)$$

(2.1) reduce to:

$$(\mu+\kappa)\left(\frac{\partial^2 u}{\partial r^2} + \frac{1}{r}\frac{\partial u}{\partial r} - \frac{u}{r^2} + \frac{\partial^2 u}{\partial z^2}\right) - \kappa\frac{\partial \phi}{\partial z} - \frac{\partial p}{\partial r} = \rho\left(u\frac{\partial u}{\partial r} + w\frac{\partial u}{\partial z}\right) \tag{5.1}$$

$$(\mu+\kappa)\left(\frac{\partial^2 w}{\partial r^2} + \frac{1}{r}\frac{\partial w}{\partial r} + \frac{\partial^2 w}{\partial z^2}\right) + \kappa\left(\frac{\partial \phi}{\partial r} + \frac{\phi}{r}\right) - \frac{\partial p}{\partial z} = \rho\left(u\frac{\partial w}{\partial r} + w\frac{\partial w}{\partial z}\right) \tag{5.2}$$

$$\gamma\left(\frac{\partial^2 \phi}{\partial r^2} + \frac{1}{r}\frac{\partial \phi}{\partial r} - \frac{\phi}{r^2} + \frac{\partial^2 \phi}{\partial z^2}\right) + \kappa\left(\frac{\partial u}{\partial z} - \frac{\partial w}{\partial r}\right) - 2\kappa\phi = \rho j\left(u\frac{\partial \phi}{\partial r} + w\frac{\partial \phi}{\partial z}\right) \tag{5.3}$$

†The dimensions of the parameters involved are as follows:

$$[\mu, \kappa] = ML^{-1}T^{-1}, \qquad [\gamma] = MLT^{-1}, \qquad [a] = T^{-1}, \qquad [j] = L^2, \qquad [\rho] = ML^{-3}.$$

$$\frac{\partial u}{\partial r}+\frac{u}{r}+\frac{\partial w}{\partial z}=0. \tag{5.4}$$

We seek solutions such that $v_r = v_z = 0$ on $z = 0$, $v_\theta = 0$ on $z = 0$, and such that the flow tends to one with potential $(1/2)a(r^2-2z^2)$ as $z\to\infty$, with a consequent pressure distribution $p = p_0-(1/2)\rho a^2(r^2+4z^2)$. Following the method used in Section 3, we set

$$\eta=\frac{z}{\lambda},\qquad \lambda^2=\frac{\mu+\kappa}{\rho a} \tag{5.5}$$

$$u=arf'(\eta),\qquad w=-2a\lambda f(\eta),\qquad \phi=\frac{\rho a^2\lambda}{\kappa}g(\eta) \tag{5.6}$$

then (5.1) and (5.3) reduce to

$$f'''(\eta)+2f(\eta)f''(\eta)-f'^2(\eta)-g'(\eta)+1=0 \tag{5.7}$$

$$g''(\eta)+c_1f''(\eta)-2c_2g(\eta)=c_3(f'(\eta)g(\eta)-2f(\eta)g'(\eta)) \tag{5.8}$$

where, as previously,

$$c_1=\frac{\kappa^2}{\gamma\rho a},\qquad c_2=\frac{(\mu+\kappa)\kappa}{\gamma\rho a},\qquad c_3=\frac{(\mu+\kappa)j}{\gamma}. \tag{5.9}$$

The boundary conditions are

$$f(0)=f'(0)=0,\qquad f'(\infty)=1,\qquad g(\infty)=0$$

and (a) $$g(0)=0 \tag{5.10}$$

OR (b) $$g'(0)=0.$$

Equations (5.7) and (5.8) were integrated, using the Runge–Kutta method, as outlined in Section 4, with boundary conditions (5.10a) or (5.10b).

6. DISCUSSION OF RESULTS

Equations (3.15) and (5.7–8) were integrated numerically, using boundary conditions (3.18) and

$$\begin{aligned} &g(0)=0 \quad \text{(strong interaction)}\\ \text{OR}\qquad &g'(0)=0 \quad \text{(weak interaction).}\end{aligned} \tag{6.1}$$

The values of the parameters† were chosen to represent possibly typical values of the material constants as follows:

$$\begin{aligned} c_1&=0.1,\quad 0.25,\quad 0.5,\\ c_2&=0.75,\quad 1.0,\quad 1.5,\\ c_3&=0.1,\quad 0.25,\quad 0.5.\end{aligned} \tag{6.2}$$

†The parameters used by Peddieson and McNitt[1] were

$$\Delta=\frac{\kappa}{\mu},\qquad \lambda=\frac{\gamma}{\mu I},\qquad \sigma=\frac{\kappa L}{\rho UI}$$

where $I = j$ in the notation of our paper, and $U = aL$. These parameters are related to ours as follows:

$$c_1=\Delta\sigma/\lambda,\qquad c_2=(1+\Delta)\sigma/\lambda,\qquad c_3=(1+\Delta)/\lambda.$$

However, we have used λ differently elsewhere as defined in (3.14).

The consequent values of $f''(0)$ and $g'(0)$, or $g(0)$, respectively, for all 108 runs, are given in Table 1. Numerical values of $f'(\eta)$, $f''(\eta)$ and $g(\eta)$ are given in Tables 2 and 3, for a particular set of values of c_1, c_2 and c_3, and compared with the solution for classical viscous flow ([8], p. 90). Typical sets of solutions, showing the effects of the parameters c_1, c_2, c_3, varying one at a time, are given in graphical form in Figs. 1–24. In Figs. 13–15, it was found convenient to multiply the vertical difference between the central graph and those above and below by a factor of 10, as indicated in the figures.

For all values of c_1, c_2 and c_3 considered, it was found that the profile of $g(\eta)$ was

(1) *raised* as c_1 was increased and

(2) lowered as c_2 or c_3 were increased *regardless* of whether the boundary condition was $g(0) = 0$ or $g'(0) = 0$.

On the other hand, the profile of $f'(\eta)$ was affected *differently* depending on the boundary condition. In particular the profile of $f'(\eta)$ was

(1a) *lowered* for small values of η, but *raised* for larger values of η as c_1 was *increased*, when $g(0) = 0$, but

(1b) *raised* for all values of η, as c_1 was *increased*, when $g'(0) = 0$.

(2a) *raised* for small values of η, but *lowered* for larger values of η as c_2 was *increased*, when $g(0) = 0$, but

(2b) *lowered* for all values of η, as c_2 was *increased*, when $g'(0) = 0$.

(3) *raised* for small values of η, but *lowered* for large values of η, as c_3 was *increased*, *regardless* of whether the boundary condition was $g(0) = 0$ or $g'(0) = 0$.

Comparative profiles of $f'(\eta)$ for micropolar flow, with $g(0) = 0$ and $g'(0) = 0$, and for classical viscous flow ([8], p. 90) are shown graphically in Figs. 25 and 26.

Table 1. $g(0) = 0$, $g'(0) = 0$

			PLANE FLOW		AXISYMMETRIC FLOW		PLANE FLOW		AXISYMMETRIC FLOW	
c_1	c_2	c_3	f"(0)	g'(0)	f"(0)	g'(0)	f"(0)	g(0)	f"(0)	g(0)
0.1	0.75	0.1	1.22186	-0.05315	1.30136	0.05583	1.24523	-0.04298	1.32568	0.04480
		0.25	1.22239	-0.05229	1.30207	0.05470	1.24534	-0.04126	1.32588	0.04243
		0.5	1.22315	-0.05101	1.30303	0.05306	1.24541	-0.03880	1.32596	0.03917
	1.0	0.1	1.22323	-0.04955	1.30262	0.05226	1.24338	-0.03486	1.32370	0.03657
		0.25	1.22360	-0.04893	1.30314	0.05144	1.24349	-0.03384	1.32388	0.03514
		0.5	1.22416	-0.04798	1.30386	0.05021	1.24358	-0.03232	1.32401	0.03309
	1.5	0.1	1.22503	-0.04439	1.30433	0.04705	1.24108	-0.02560	1.32122	0.02704
		0.25	1.22526	-0.04402	1.30464	0.04656	1.24116	-0.02513	1.32134	0.02638
		0.5	1.22559	-0.04343	1.30509	0.04579	1.24125	-0.02440	1.32148	0.02537
0.25	0.75	0.1	1.20559	-0.13289	1.28534	0.13961	1.26474	-0.10873	1.34686	0.11322
		0.25	1.20695	-0.13075	1.28715	0.13681	1.26501	-0.10432	1.34734	0.10715
		0.5	1.20887	-0.12757	1.28956	0.13271	1.26517	-0.09802	1.34752	0.09883
	1.0	0.1	1.20905	-0.12389	1.28852	0.13067	1.26000	-0.08808	1.34178	0.09231
		0.25	1.21001	-0.12235	1.28983	0.12865	1.26024	-0.08547	1.34221	0.08868
		0.5	1.21142	-0.12000	1.29166	0.12559	1.26048	-0.08159	1.34254	0.08344
	1.5	0.1	1.21360	-0.11099	1.29280	0.11765	1.25409	-0.06456	1.33540	0.06817
		0.25	1.21417	-0.11006	1.29359	0.11643	1.25428	-0.06336	1.33572	0.06649
		0.5	1.21503	-0.10860	1.29475	0.11452	1.25450	-0.06150	1.33607	0.06392
0.5	0.75	0.1	1.17808	-0.26583	1.25833	0.27933	1.29889	-0.22190	1.38377	0.23059
		0.25	1.18087	-0.26162	1.26201	0.27381	1.29941	-0.21269	1.38471	0.21797
		0.5	1.18479	-0.25531	1.26691	0.26568	1.29967	-0.19957	1.38494	0.20072
	1.0	0.1	1.18511	-0.24783	1.26477	0.26145	1.28891	-0.17935	1.37316	0.18770
		0.25	1.18708	-0.24480	1.26743	0.25747	1.28939	-0.17394	1.37402	0.18019
		0.5	1.18995	-0.24014	1.27114	0.25139	1.28983	-0.16589	1.37460	0.16934
	1.5	0.1	1.19435	-0.22201	1.27343	0.23537	1.27654	-0.13104	1.35986	0.13825
		0.25	1.19551	-0.22019	1.27503	0.23299	1.27691	-0.12857	1.36050	0.13479
		0.5	1.19725	-0.21731	1.27738	0.22920	1.27736	-0.12474	1.36118	0.12952
Classical Flow			1.2326		1.3120					

Table 2. Plane flow: $c_1 = 0.5$, $c_2 = 0.75$, $c_3 = 0.1$

	Micropolar: g(0) = 0			Micropolar: g'(0) = 0			Classical	
η	f'(η)	f"(η)	-g(η)	f'(η)	f"(η)	-g(η)	f'(η)	f"(η)
0	0	1.178081	0	0	1.298887	0.221902	0	1.2326
0.2	0.220284	1.022179	0.042370	0.239494	1.095313	0.216251	0.2266	1.0345
0.4	0.408317	0.857851	0.066788	0.438295	0.894162	0.201831	0.4145	0.8463
0.6	0.563663	0.697011	0.078066	0.598074	0.706630	0.181970	0.5663	0.6752
0.8	0.687932	0.548259	0.080175	0.722350	0.540053	0.159364	0.6859	0.5251
1.0	0.784146	0.417142	0.076298	0.815763	0.398419	0.136084	0.7779	0.3980
1.2	0.856159	0.306524	0.068896	0.883463	0.282917	0.113625	0.8467	0.2938
1.4	0.908167	0.217032	0.059795	0.930608	0.192563	0.092976	0.8968	0.2110
1.6	0.944310	0.147581	0.050272	0.961997	0.124835	0.074699	0.9323	0.1474
1.8	0.968385	0.095916	0.041160	0.981821	0.076302	0.059023	0.9568	0.1000
2.0	0.983668	0.059139	0.032943	0.993544	0.043181	0.045932	0.9732	0.0658
2.2	0.992826	0.034160	0.025844	0.999873	0.021786	0.035244	0.9839	0.0420
2.4	0.997921	0.018044	0.019911	1.002811	0.008832	0.026682	0.9905	0.0260
2.6	1.000459	0.008237	0.015075	1.003769	0.001611	0.019928	0.9946	0.0156
2.8	1.001486	0.002675	0.011208	1.003679	-0.001957	0.016659	0.9970	0.0090
3.0	1.001691	-0.000199	0.008154	1.003111	-0.003369	0.010577	0.9984	0.0051
3.2	1.001495	-0.001485	0.005754	1.002388	-0.003630	0.007416	0.9992	0.0028
3.4	1.001138	-0.001912	0.003863	1.001677	-0.003367	0.004951	0.9996	0.0014
3.6	1.000737	-0.001933	0.002352	1.001037	-0.002939	0.002996	0.9998	0.0007
3.8	1.000354	-0.001805	0.001113	1.000484	-0.002532	0.001400	0.9999	0.0004
4.0	1.000000	-0.001663	0.000054	1.000001	-0.002225	0.000040	1.0000	0.0002

Table 3. Axisymmetric flow: $c_1 = 0.5$, $c_2 = 0.75$, $c_3 = 0.1$

	Micropolar: g(0) = 0			Micropolar: g'(0) = 0			Classical	
η	f'(η)	f"(η)	g(η)	f'(η)	f"(η)	g(η)	f'(η)	f"(η)
0	0	1.258327	0	0	1.383765	0.230586	0	1.3120
0.2	0.236467	1.102731	0.044283	0.256332	1.177707	0.224351	0.1755	1.1705
0.4	0.439915	0.929578	0.069113	0.470585	0.964332	0.208228	0.3311	1.0298
0.6	0.607786	0.748825	0.079502	0.642219	0.753364	0.185747	0.4669	0.8910
0.8	0.739726	0.572322	0.079786	0.772875	0.556551	0.159987	0.5833	0.7563
1.0	0.837792	0.411919	0.073635	0.866536	0.385536	0.133514	0.6811	0.6283
1.2	0.906201	0.276987	0.064012	0.929130	0.246781	0.108301	0.7614	0.5097
1.4	0.950623	0.172446	0.053142	0.967646	0.144291	0.085672	0.8258	0.4031
1.6	0.977208	0.098207	0.042534	0.989070	0.075051	0.066334	0.8761	0.3100
1.8	0.991655	0.050146	0.033063	0.999470	0.032839	0.050470	0.9142	0.2315
2.0	0.998593	0.022001	0.025110	1.003488	0.010015	0.037889	0.9422	0.1676
2.2	1.001343	0.007300	0.018721	1.004275	-0.000518	0.028183	0.9622	0.1175
2.4	1.002031	0.000659	0.013749	1.003716	-0.004219	0.020861	0.9760	0.0798
2.6	1.001868	-0.001719	0.009962	1.002783	-0.004672	0.015438	0.9853	0.0523
2.8	1.001452	-0.002152	0.007118	1.001960	-0.003901	0.011490	0.9912	0.0331
3.0	1.001036	-0.001870	0.004995	1.001221	-0.002878	0.008666	0.9949	0.0202
3.2	1.000697	-0.001433	0.003410	1.000732	-0.001977	0.006695	0.9972	0.0120
3.4	1.000443	-0.001048	0.002220	1.000401	-0.001286	0.005370	0.9985	0.0068
3.6	1.000255	-0.000763	0.001313	1.000189	-0.000785	0.004540	0.9992	0.0037
3.8	1.000114	-0.000571	0.000603	1.000061	-0.000425	0.004095	0.9996	0.0020
4.0	1.000006	-0.000449	0.000027	1.000000	-0.000163	0.003961	0.9998	0.0010

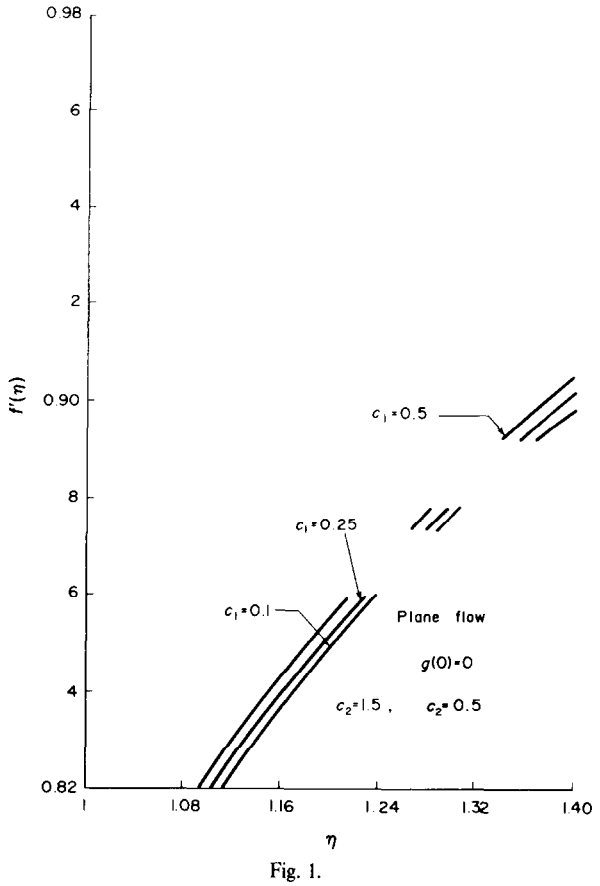
0.98
6
4
2
0.90
8
6
4
0.82
f'(η)
1
1.08
1.16
1.24
1.32
1.40
η
c₁=0.5
c₁=0.25
c₁=0.1
Plane flow
g(0)=0
c₂=1.5 , c₂=0.5

Fig. 1.

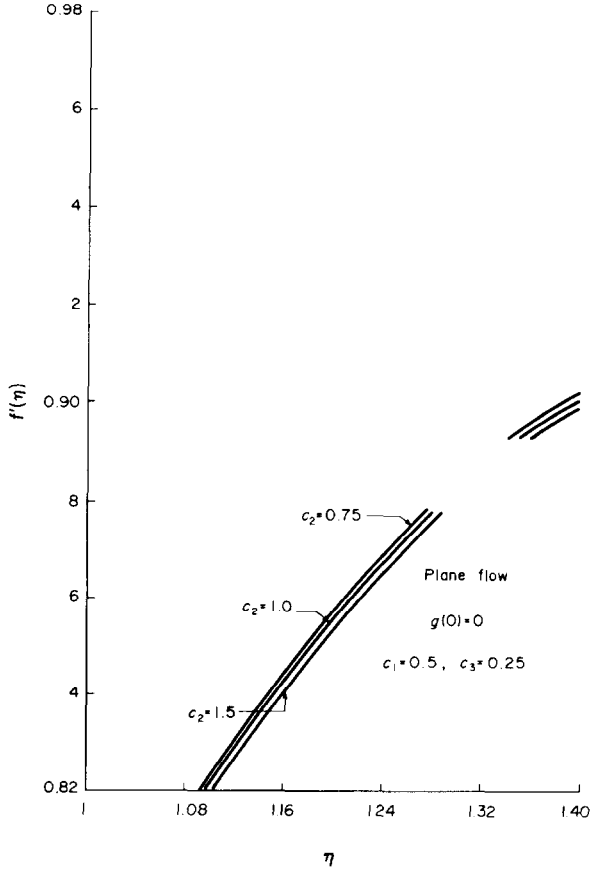
0.98
6
4
2
0.90
8
6
4
0.82
f'(η)
1
1.08
1.16
1.24
1.32
1.40
η
c₂=0.75
c₂=1.0
c₂=1.5
Plane flow
g(0)=0
c₁=0.5 , c₃=0.25

Fig. 2.

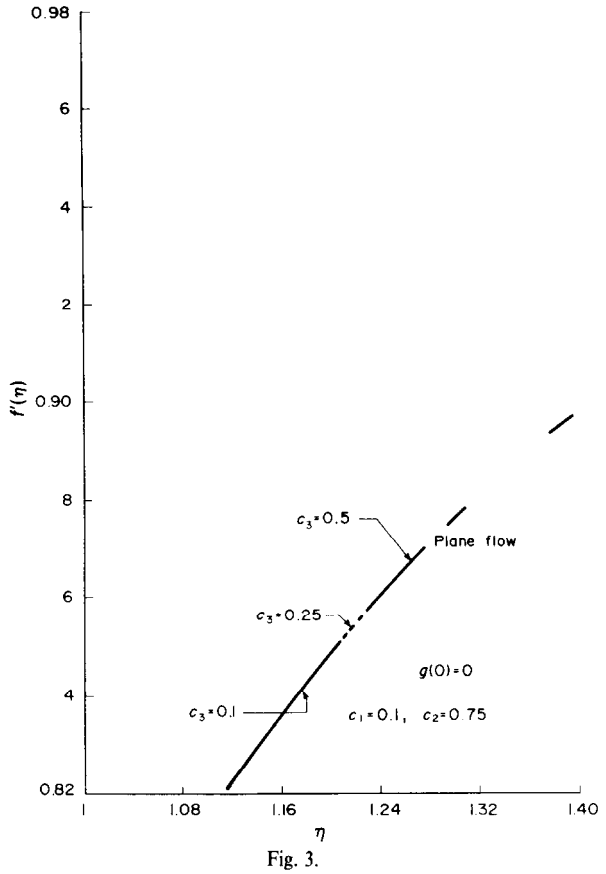
0.98
6
4
2
0.90
8
6
4
0.82
f'(η)
1
1.08
1.16
1.24
1.32
1.40
η
c3=0.5
Plane flow
c3=0.25
g(0)=0
c3=0.1
c1=0.1, c2=0.75

Fig. 3.

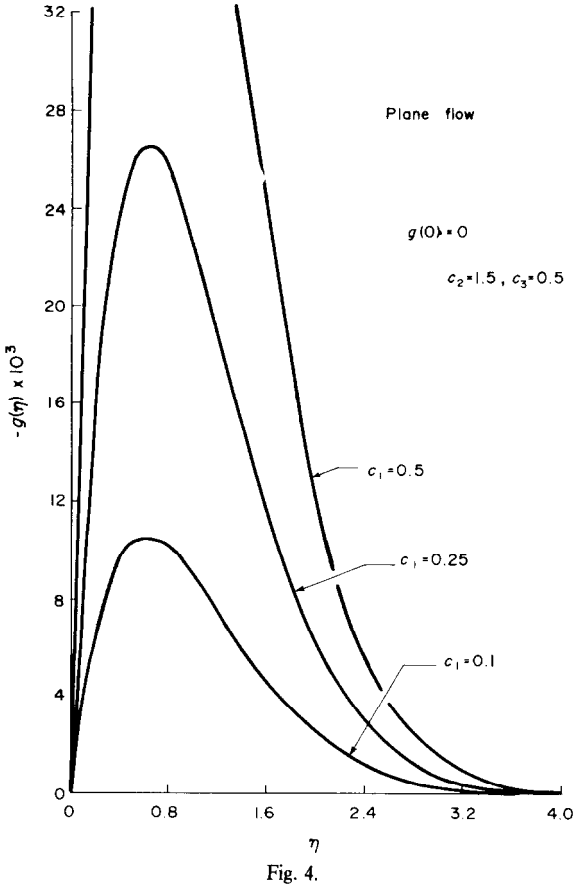
32
28
24
20
16
12
8
4
0
-g(η) x 10^3
0
0.8
1.6
2.4
3.2
4.0
η
Plane flow
g(0)=0
c2=1.5, c3=0.5
c1=0.5
c1=0.25
c1=0.1

Fig. 4.

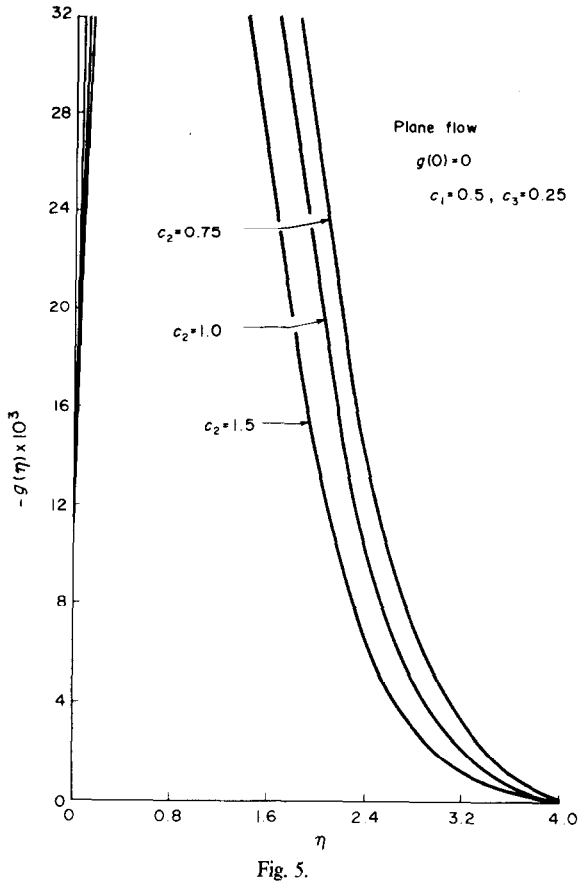
Plane flow
g(0)=0
c1=0.5, c3=0.25
c2=0.75
c2=1.0
c2=1.5
-g(η) x 10^3
η
0
4
8
12
16
20
24
28
32
0.8
1.6
2.4
3.2
4.0

Fig. 5.

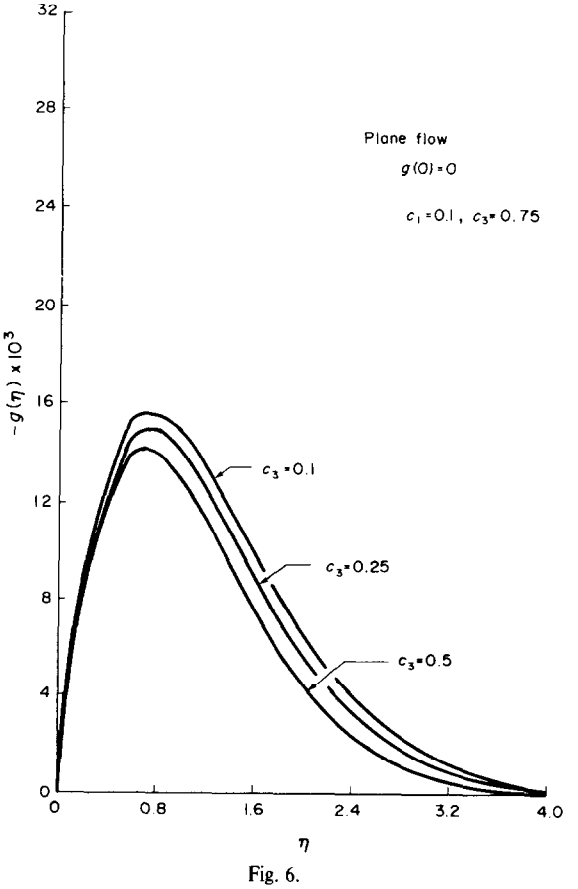
Plane flow
g(0)=0
c1=0.1, c3=0.75
c3=0.1
c3=0.25
c3=0.5
-g(η) x 10^3
η
0
4
8
12
16
20
24
28
32
0.8
1.6
2.4
3.2
4.0

Fig. 6.

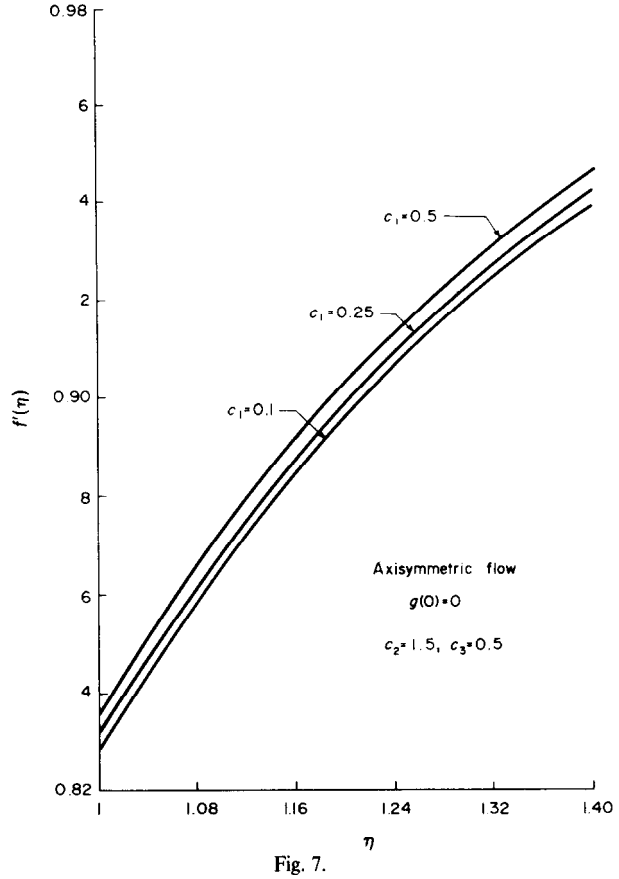
0.98
6
4
2
0.90
8
6
4
0.82
1
1.08
1.16
1.24
1.32
1.40
η
f'(η)
c₁=0.5
c₁=0.25
c₁=0.1
Axisymmetric flow
g(0)=0
c₂=1.5, c₃=0.5

Fig. 7.

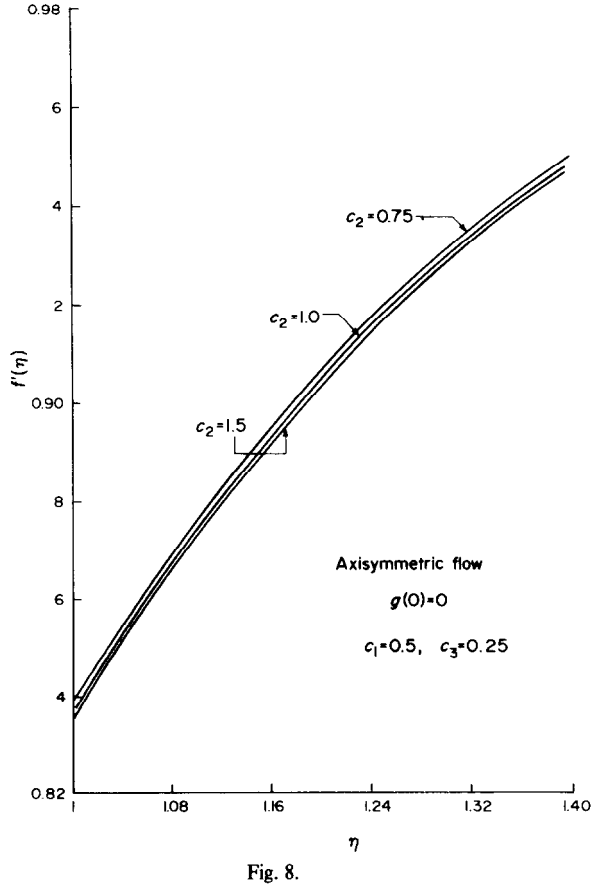
0.98
6
4
2
0.90
8
6
4
0.82
1
1.08
1.16
1.24
1.32
1.40
η
f'(η)
c₂=0.75
c₂=1.0
c₂=1.5
Axisymmetric flow
g(0)=0
c₁=0.5, c₃=0.25

Fig. 8.

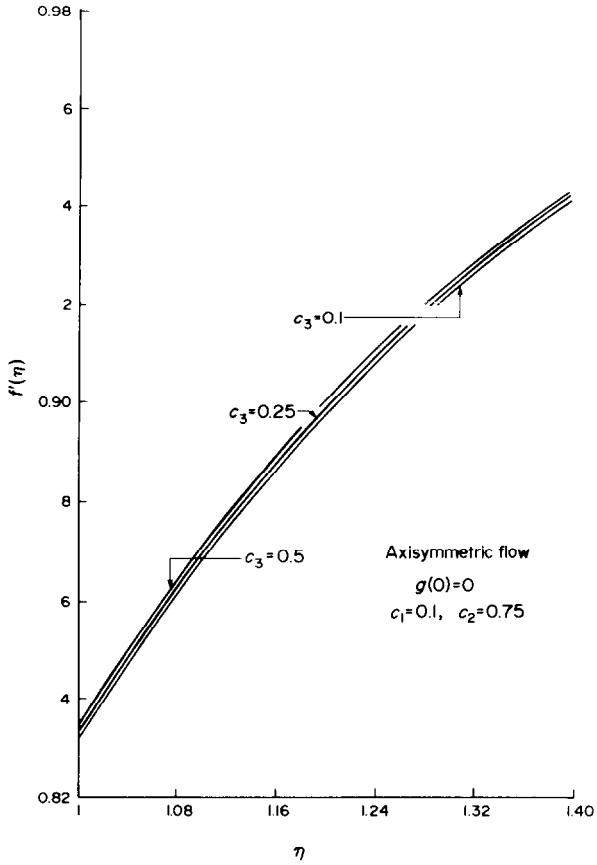
0.98
6
4
2
0.90
8
6
4
0.82
f'(η)
c3=0.1
c3=0.25
c3=0.5
Axisymmetric flow
g(0)=0
c1=0.1, c2=0.75
1
1.08
1.16
1.24
1.32
1.40
η

Fig. 9.

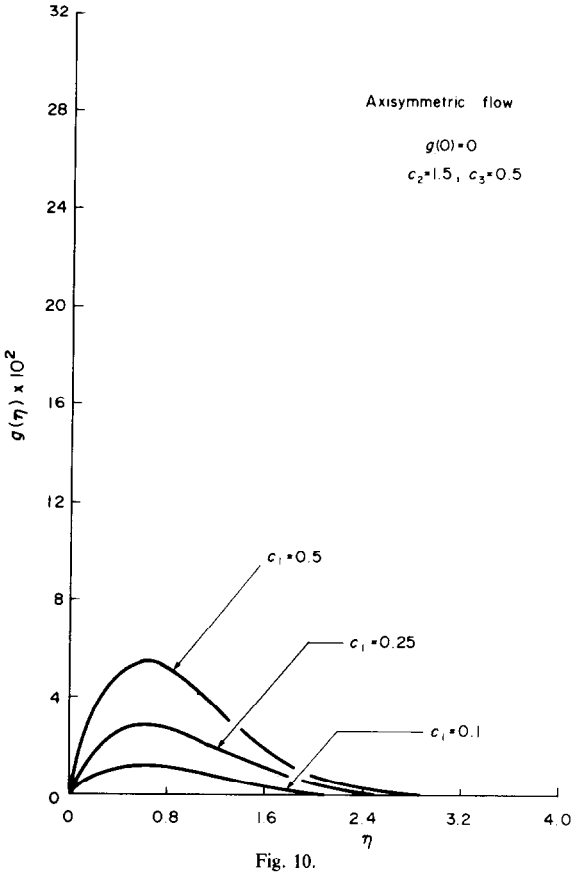
32
28
24
20
16
12
8
4
0
g(η) x 10²
Axisymmetric flow
g(0)=0
c2=1.5, c3=0.5
c1=0.5
c1=0.25
c1=0.1
0
0.8
1.6
2.4
3.2
4.0
η

Fig. 10.

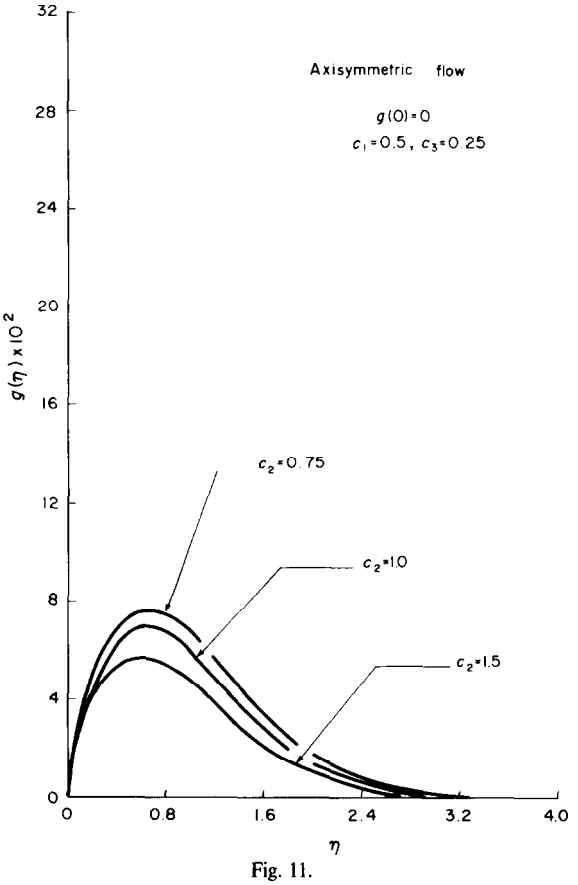
Axisymmetric flow
g(0)=0
c1=0.5, c3=0.25
c2=0.75
c2=1.0
c2=1.5
g(η) x 10^2
η
0
0.8
1.6
2.4
3.2
4.0
4
8
12
16
20
24
28
32

Fig. 11.

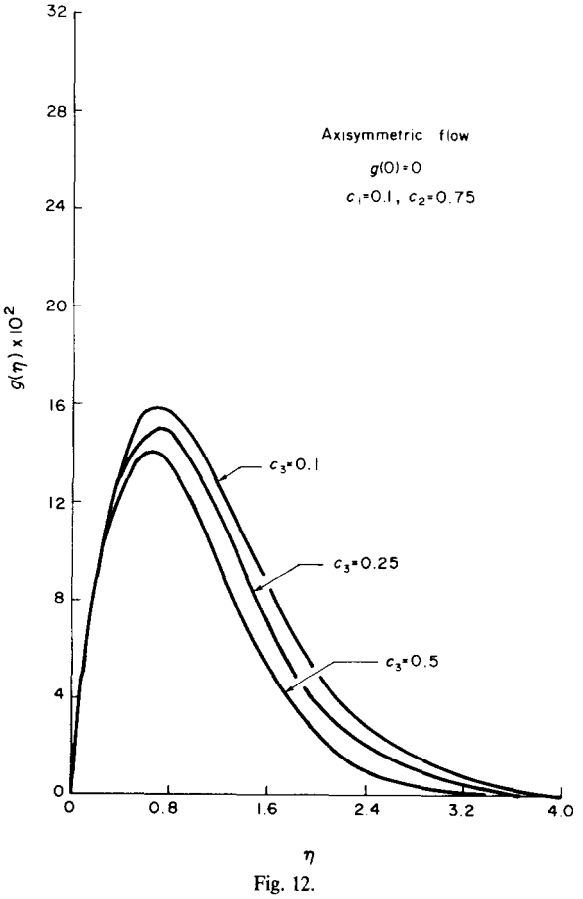
Axisymmetric flow
g(0)=0
c1=0.1, c2=0.75
c3=0.1
c3=0.25
c3=0.5
g(η) x 10^2
η
0
0.8
1.6
2.4
3.2
4.0
4
8
12
16
20
24
28
32

Fig. 12.

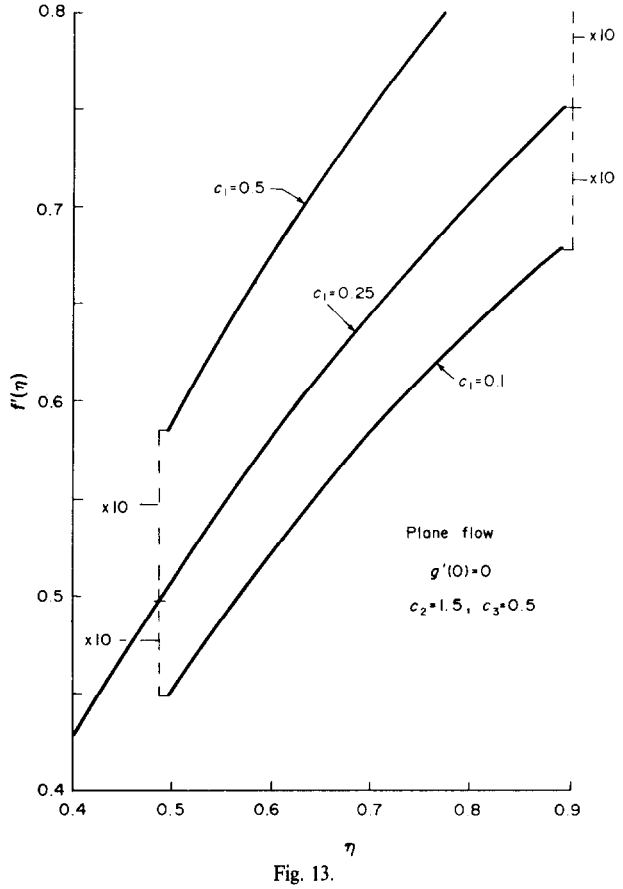
0.8
0.7
0.6
0.5
0.4
0.4
0.5
0.6
0.7
0.8
0.9
f'(η)
η
x10
x10
x10
x10
c1=0.5
c1=0.25
c1=0.1
Plane flow
g'(0)=0
c2=1.5, c3=0.5

Fig. 13.

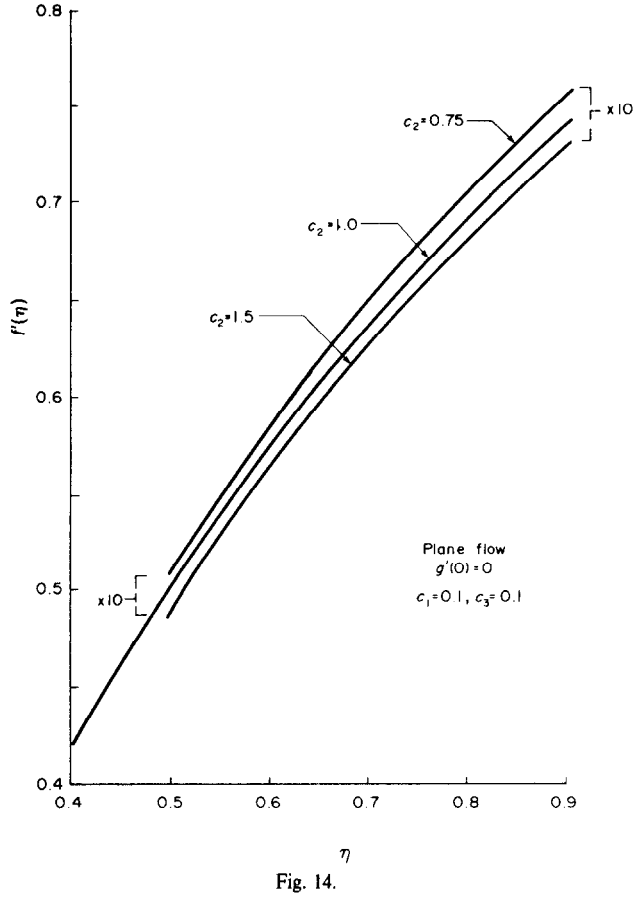
0.8
0.7
0.6
0.5
0.4
0.4
0.5
0.6
0.7
0.8
0.9
f'(η)
η
x10
x10
c2=0.75
c2=1.0
c2=1.5
Plane flow
g'(0)=0
c1=0.1, c3=0.1

Fig. 14.

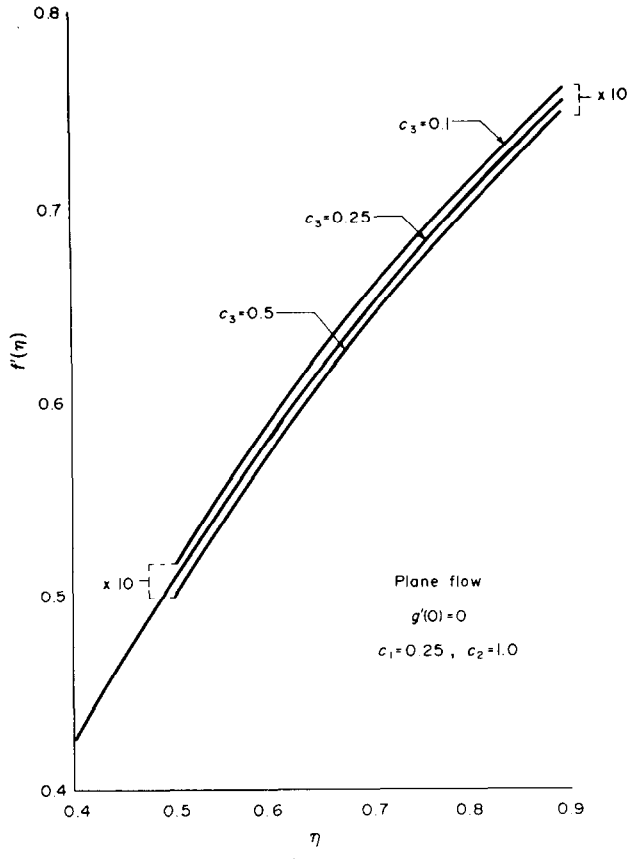
0.8
0.7
0.6
0.5
0.4
f'(η)
x 10
x 10
c3=0.1
c3=0.25
c3=0.5
Plane flow
g'(0)=0
c1=0.25, c2=1.0
0.4
0.5
0.6
0.7
0.8
0.9
η

Fig. 15.

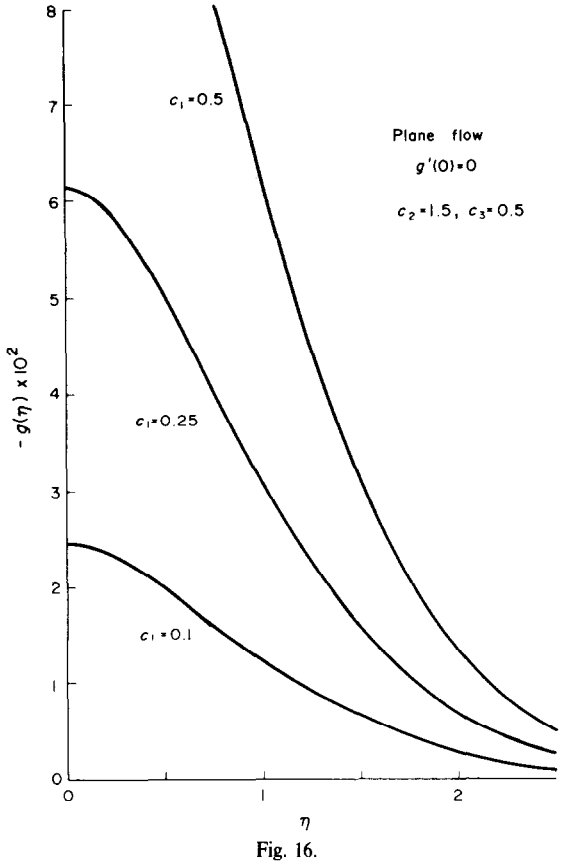
8
7
6
5
4
3
2
1
0
- g(η) x 10²
c1=0.5
c1=0.25
c1=0.1
Plane flow
g'(0)=0
c2=1.5, c3=0.5
0
1
2
η

Fig. 16.

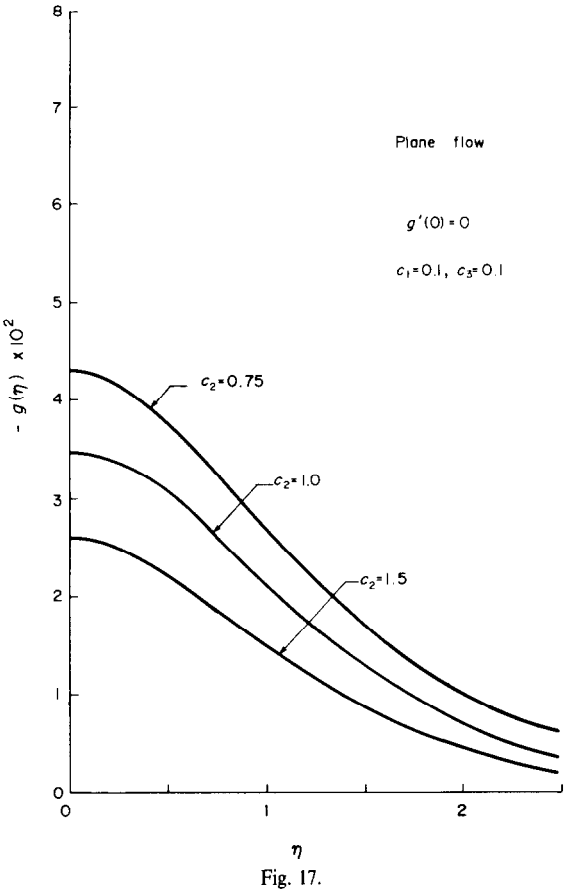
Plane flow
g'(0) = 0
c1=0.1, c3=0.1
c2=0.75
c2=1.0
c2=1.5
- g(η) x 10²
η

Fig. 17.

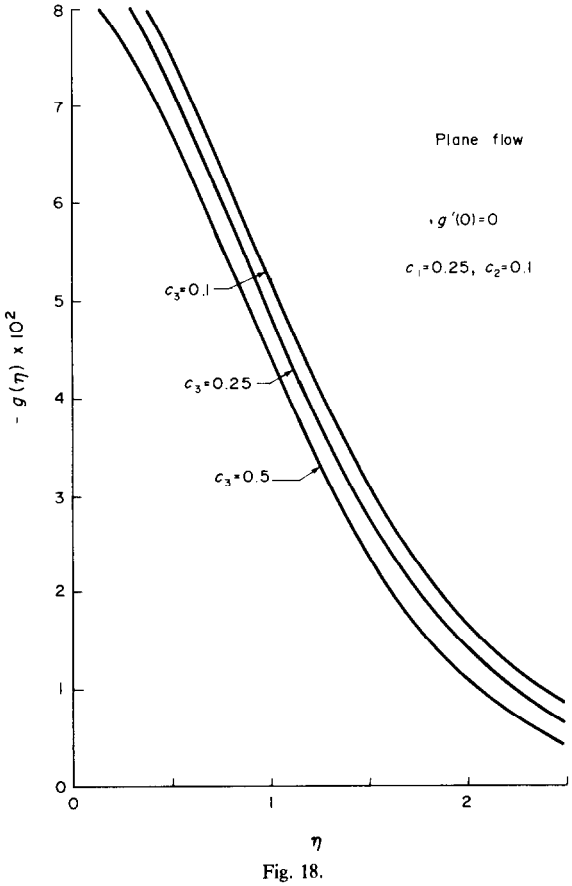
Plane flow
g'(0)=0
c1=0.25, c2=0.1
c3=0.1
c3=0.25
c3=0.5
- g(η) x 10²
η

Fig. 18.

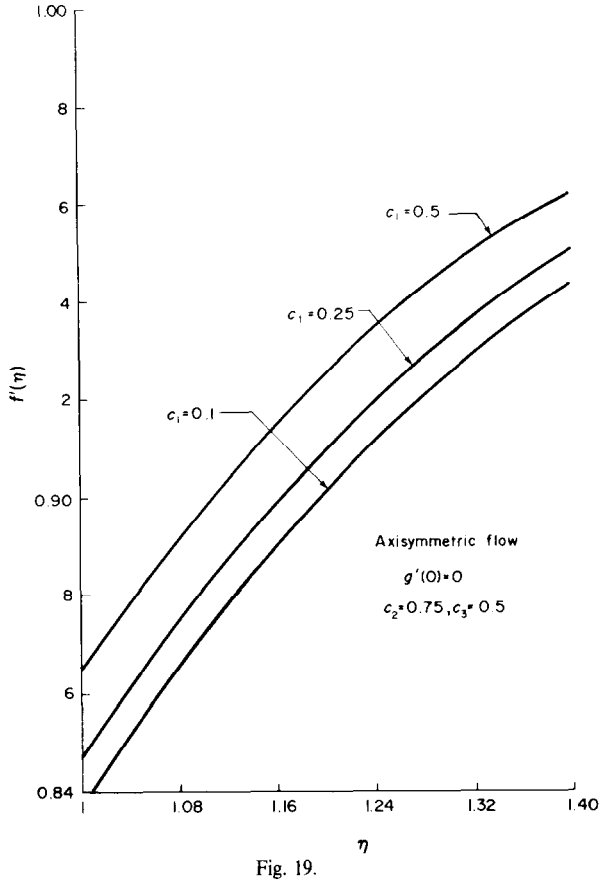
1.00
8
6
4
2
0.90
8
6
0.84
f'(η)
c₁=0.5
c₁=0.25
c₁=0.1
Axisymmetric flow
g'(0)=0
c₂=0.75, c₃=0.5
1
1.08
1.16
1.24
1.32
1.40
η

Fig. 19.

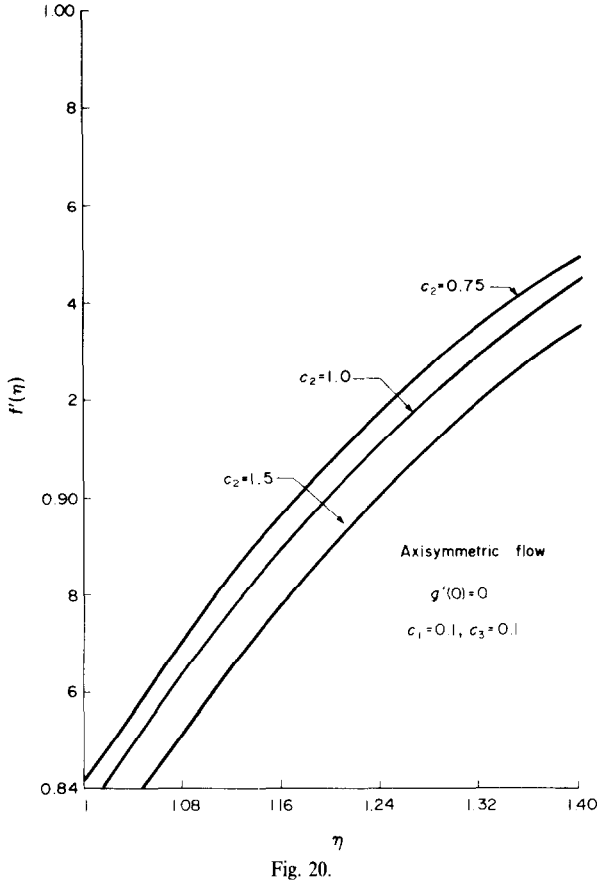
1.00
8
6
4
2
0.90
8
6
0.84
f'(η)
c₂=0.75
c₂=1.0
c₂=1.5
Axisymmetric flow
g'(0)=0
c₁=0.1, c₃=0.1
1
1.08
1.16
1.24
1.32
1.40
η

Fig. 20.

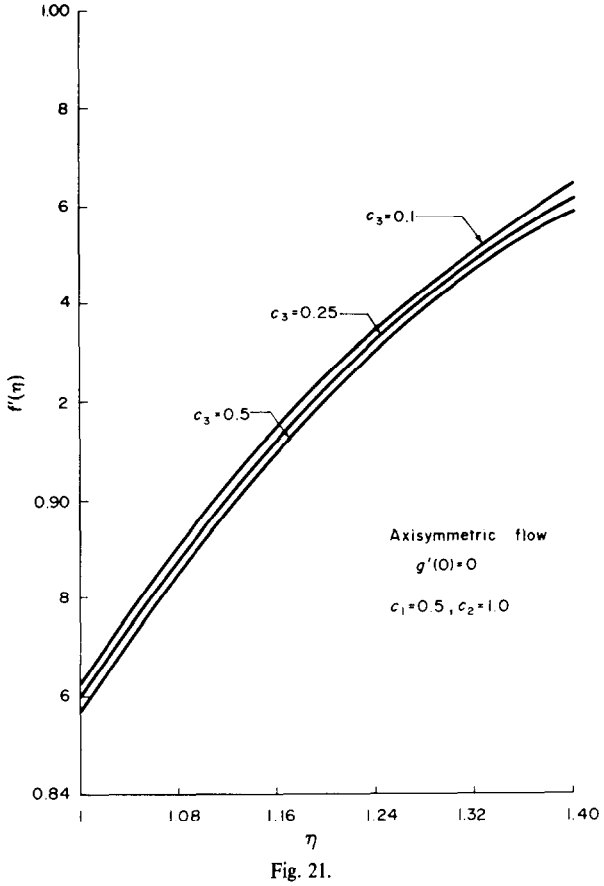
1.00
8
6
4
2
0.90
8
6
0.84
f'(η)
c3=0.1
c3=0.25
c3=0.5
Axisymmetric flow
g'(0)=0
c1=0.5, c2=1.0
1
1.08
1.16
1.24
1.32
1.40
η

Fig. 21.

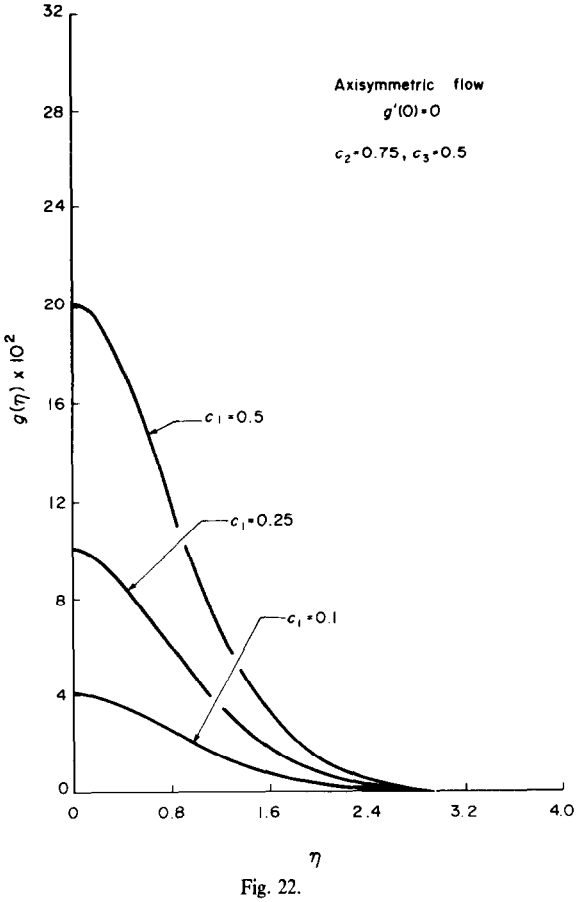
32
28
24
20
16
12
8
4
0
g(η) x 10²
Axisymmetric flow
g'(0)=0
c2=0.75, c3=0.5
c1=0.5
c1=0.25
c1=0.1
0
0.8
1.6
2.4
3.2
4.0
η

Fig. 22.

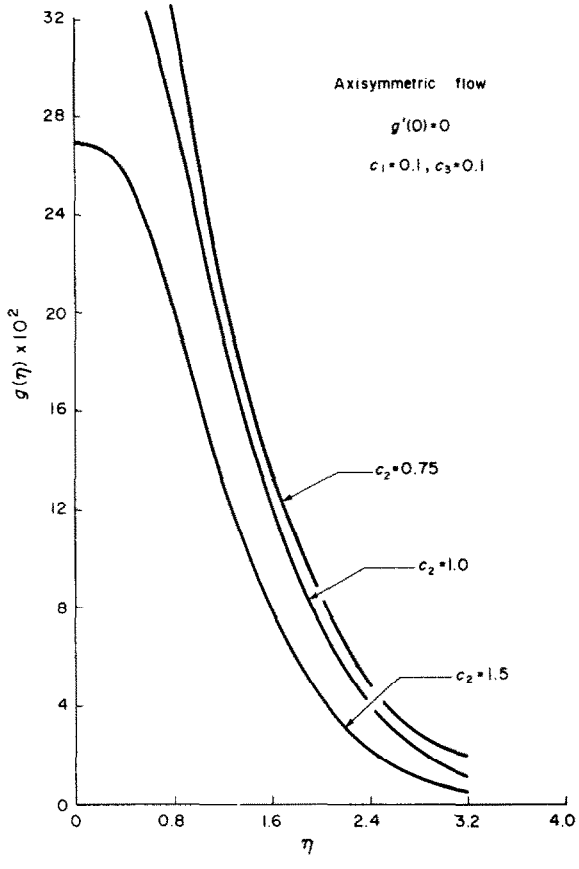
Axisymmetric flow
g'(0)=0
c1=0.1, c3=0.1
c2=0.75
c2=1.0
c2=1.5
g(η) x 10²
η
0
4
8
12
16
20
24
28
32
0.8
1.6
2.4
3.2
4.0

Fig. 23.

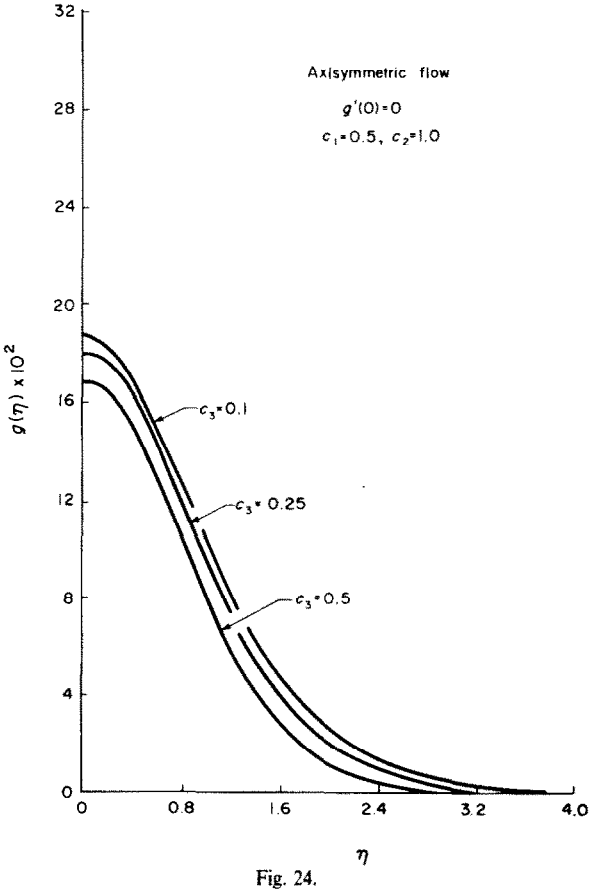
Axisymmetric flow
g'(0)=0
c1=0.5, c2=1.0
c3=0.1
c3=0.25
c3=0.5
g(η) x 10²
η
0
4
8
12
16
20
24
28
32
0.8
1.6
2.4
3.2
4.0

Fig. 24.

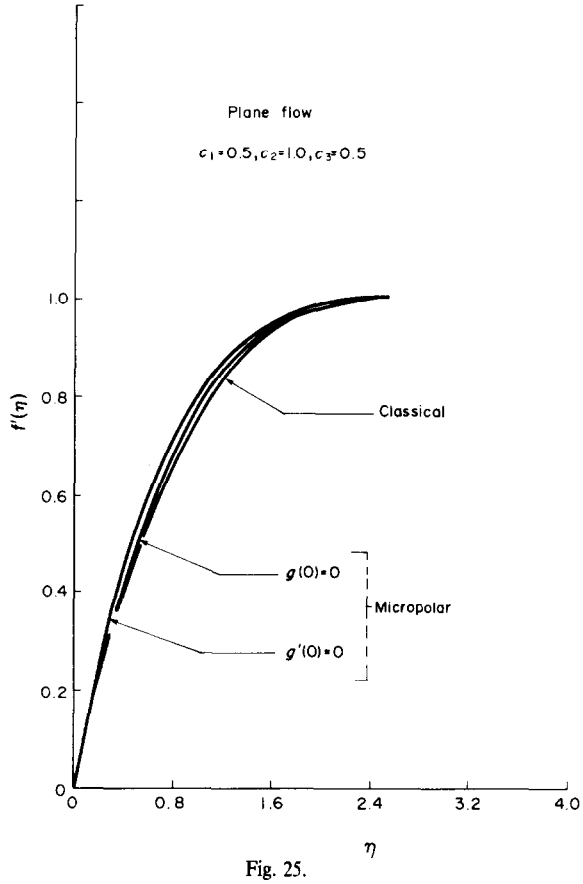
Plane flow
$c_1=0.5, c_2=1.0, c_3=0.5$
Classical
$g(0)=0$
$g'(0)=0$
Micropolar
$f'(\eta)$
η
0
0.2
0.4
0.6
0.8
1.0
0.8
1.6
2.4
3.2
4.0

Fig. 25.

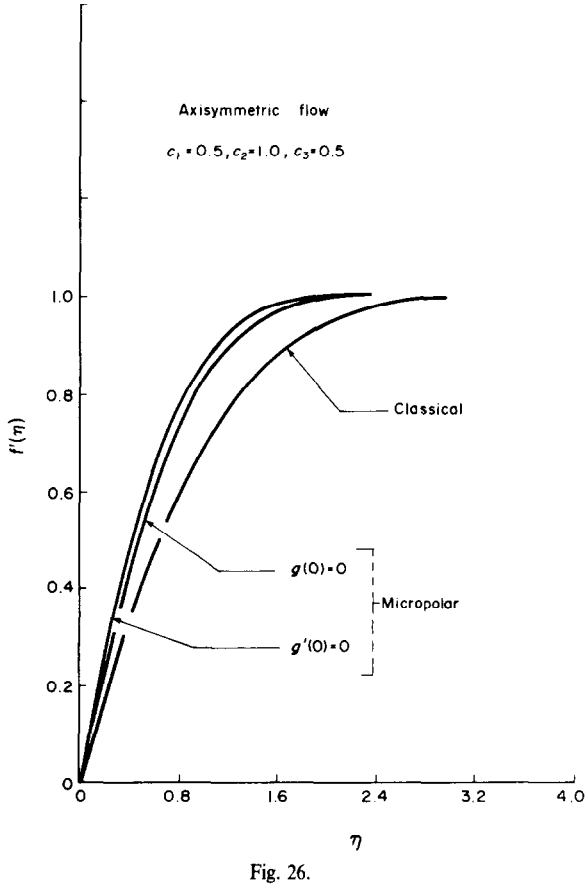
Axisymmetric flow
$c_1=0.5, c_2=1.0, c_3=0.5$
Classical
$g(0)=0$
$g'(0)=0$
Micropolar
$f'(\eta)$
η
0
0.2
0.4
0.6
0.8
1.0
0.8
1.6
2.4
3.2
4.0

Fig. 26.

As might be expected, Figs. 1–12 are qualitatively similar to Figs. 1–6 of Peddieson and McNitt[1]. When c_1 is sufficiently large, in particular $c_1 \geq 0.5$, it is found that the graph of $f'(\eta)$ exceeds unity and then levels out with $f'(\infty) = 1$; a result which is also apparent in ([1], Fig. 3). The horizontal shearing stress, in plane flow, from (2.2) and (3.13) is

$$t_{21} = \frac{(\mu + \kappa) ax}{\lambda} [f''(\eta) + g(\eta)]. \tag{6.3}$$

In the case considered in Table 2, it is clear that the shearing stress changes sign about $\eta = 2.3$, when $g(0) = 0$, and about $\eta = 1.9$, when $g'(0) = 0$. Thus there is a reversal of shearing stress in plane flow when c_1 is large enough. Similar considerations apply to axisymmetric flow.

In all cases, the *maximum* value of $g(\eta)$ attained when $g'(0) = 0$ was greater than that when $g(0) = 0$. The ratio of the two varied from as little as 1.2 to as much as 5.

When $g'(0) = 0$, it is easily seen that $(2\phi + u_y)_{y=0} = 2((c_2/c_1) g(0) - f''(0))$. The value obtained from Table 2, for example, is 0.9660.

Lastly, we remark on the ratio of spin to vorticity. In plane flow it follows from (3.13) that

$$\frac{\phi}{\omega} = -\left(\frac{\mu + \kappa}{\kappa}\right) \frac{g(\eta)}{f''(\eta)} \tag{6.4}$$

where $\omega = v_x - u_y$ and $(\mu + \kappa)/\kappa = (c_2/c_1)$.
In axisymmetric flow the value is the same, but the sign is positive.

From Tables 2 and 3, it appears that ϕ and ω are of the same order of magnitude in most of the flow.

7. CONCLUSION

The numerical results obtained may serve to determine, in conjunction with experiments, which, if either, of the extreme boundary conditions is the more appropriate to apply to a real fluid exhibiting micropolar behaviour.

Acknowledgement—We wish to thank the National Research Council of Canada (Grant Number A3098) for the support of one author (G.S.G.) during the writing of this paper.

REFERENCES

1. J. Peddieson and R. P. McNitt, *Recent Advances in Engineering Science* (Edited by A. C. Eringen), Vol. 5/I, pp. 405–426. Gordon & Breach, London (1970).
2. J. Peddieson, *Int. J. Engng Sci.* **10**, 23–32 (1972).
3. G. Ahmadi, *Int. J. Engng Sci.* **14**, 639–646 (1976).
4. F. Ebert, *Chem. Engng J.* **5**, 85–92 (1973).
5. E. L. Aero, A. N. Bulygin and E. V. Kuvshinskii, *J. Appl. Math. Mech. (P.M.M.)* **29**(1), 333–346 (1965).
6. D. W. Condiff and J. S. Dahler, *Phys. Fluids* **7**(6), 842–854 (1964).
7. A. C. Eringen, *J. Math. Mech.* **16**(1), 1–18 (1966).
8. H. Schlichting, *Boundary Layer Theory*, 6th Edn. McGraw-Hill, New York (1968).
9. *Modern Computing Methods*, 2nd Edn. H.M. Stationery Office, London (1961).
10. A. C. Smith and G. S. Guram, *Letters Appl. Engng Sci.* **2**, 279–292 (1974).